Journal of Hydrology 426–427 (2012) 28–38

Contents lists available at SciVerse ScienceDirect

Journal of Hydrology

journal homepage: www.elsevier.com/locate/jhydrol

Suitability of the TRMM satellite rainfalls in driving a distributed hydrological model for water balance computations in Xinjiang catchment, Poyang lake basin

Xiang-Hu Li [a], Qi Zhang [a,*], Chong-Yu Xu [b,c]

[a] State Key Laboratory of Lake Science and Environment, Nanjing Institute of Geography and Limnology, Chinese Academy of Sciences, Nanjing 210008, China
[b] Department of Geosciences, University of Oslo, Oslo, Norway
[c] School of Geographic and Oceanographic Sciences, Nanjing University, China

ARTICLE INFO

Article history:
Received 8 September 2011
Received in revised form 21 November 2011
Accepted 8 January 2012
Available online 24 January 2012
This manuscript was handled by Konstantine P. Georgakakos, Editor-in-Chief, with the assistance of Hervé Andrieu, Associate Editor

Keywords:
Rainfall
TRMM
Hydrological process
Water balance
Distributed hydrological model
Xinjiang catchment

SUMMARY

Spatial rainfall is a key input to distributed hydrological models, and its precisions heavily affect the accuracy of stream flow predictions from a hydrological model. Traditional interpolation techniques which obtain the spatial rainfall distribution from rain gauge data have some limitations caused by data scarcity and bad quality, especially in developing countries or remote locations. Satellite-based precipitation products are expected to offer an alternative to ground-based rainfall estimates in the present and the foreseeable future. For this purpose, the quality and usefulness of satellite-based precipitation products need to be evaluated. The present study compares the difference of Tropical Rainfall Measuring Mission (TRMM) rainfall with rain gauges data at different time scales and evaluates the usefulness of the TRMM rainfall for hydrological processes simulation and water balance analysis at the Xinjiang catchment, located in the lower reaches of the Yangtze River in China. The results show at daily time step TRMM rainfall data are better at determining rain occurrence and mean values than at determining the rainfall extremes, and larger difference exists for the maximal daily and maximal 5-day rainfalls. At monthly time scale, good linear relationships between TRMM rainfall and rain gauges rainfall data are received with the determination coefficients (R^2) varying between 0.81 and 0.89 for the individual stations and 0.88 for areal average rainfall data, respectively. But the slope of regression line ranges between 0.74 for Yingtan and 0.94 for Yushan, indicating that the TRMM satellite is inclined to underestimate the monthly rainfall in this area. The simulation of daily hydrological processes shows that the Water Flow Model for Lake Catchment (WATLAC) model using conventional rain gauge data produces an overall good fit, but the simulation results using TRMM rainfall data are discontented. The evaluation results imply that the TRMM rainfall data are unsuited for daily stream flow simulation in this study area with desired precisions. However, good performance can be received using TRMM rainfall data for monthly stream flow simulations. The comparison of the simulated annual water balance components shows that the different rainfall data sources can change the volume value and proportion of water balance components to some extent, but it generally meets the need of practical use.

1. Introduction

Distributed hydrological models have become the main tool to understand the hydrological processes and solve practical hydrological and water resources problems. Physically-based distributed hydrological models can fulfill the necessity of describing spatial heterogeneity, assessing the impact of natural and human induced changes and providing detailed descriptions of the hydrological processes in watersheds to satisfy various needs in spatial modelling (Abbott and Refsgaard, 1996). However, these models require the spatially distributed data as input to reflect the heterogeneity of base information in the watersheds. The spatial rainfall is one of the key inputs for these models, and the accuracy of stream flow predictions from a hydrological model is heavily dependent on the accuracy of rainfall inputs (Gourley and Vieux, 2006), therefore, accurate estimate of the rainfall patterns over a catchment and a region is a great concern (Kurtzman et al., 2009).

Conventional estimates of daily areal rainfall can be obtained by spatial interpolation of rain gauges' data (Kurtzman et al., 2009). Various interpolation techniques have been proposed for areal rainfall estimations. The isohyetal and Thiessen polygon techniques are commonly used techniques of this kind (Guillermo et al., 1985). However, direct application of these techniques may produce inaccurate results because of the effects of topographical

* Corresponding author. Address: Nanjing Institute of Geography and Limnology, Chinese Academy of Sciences, 73 East Beijing Road, Nanjing 210008, PR China. Tel.: +86 25 86882102; fax: +86 25 57714759.
E-mail addresses: lxh8010@yahoo.com.cn (X.-H. Li), qzhang@niglas.ac.cn (Q. Zhang), c.y.xu@geo.uio.no (C.-Y. Xu).

0022-1694/$ - see front matter © 2012 Elsevier B.V. All rights reserved.
doi:10.1016/j.jhydrol.2012.01.013

variation and the limited number of available rainfall stations (Taesombat and Sriwongsitanon, 2009). The geostatistical approaches, in particular the kriging method and inverse distance weighting (IDW) technique, have been widely applied for the estimation of spatially distributed rainfall. But, their results are influenced by the heterogeneity of the random fields, and the assumption of an isotropic covariance structure in the kriging method is demonstrated to be inappropriate in several articles (Brown et al., 1994; Le et al., 1997; Kibria et al., 2002). Furthermore, most methods used for interpolating rainfall have a tendency to produce too smooth rainfall fields, i.e. to underestimate the spatial variability (Creutin and Obled, 1982; Haberland, 2007), which will affect the estimation of extreme values and undermine the strength of the distributed hydrological models (Skaugen and Andersen, 2010). At the same time, it is both economically and practically impossible to greatly increase the number of rain gages for estimating the spatial rainfall (Taesombat and Sriwongsitanon, 2009). Alternatively, the incorporation of satellite-based and weather radar-based (He et al., 2011) rainfall estimates in hydrological modelling has the potential to improve our capability to reduce uncertainty in rainfall inputs (Sawunyama and Hughes, 2008).

Recent development in global and regional satellite-based precipitation products has greatly improved their applicability as input to large-scale distributed hydrological models (Stisen and Sandholt, 2010) and are expected to offer an alternative to ground-based rainfall estimates in the present and the foreseeable future (Sawunyama and Hughes, 2008). Such data are especially valuable in developing countries or remote locations, where conventional rain gauge data are sparse or of bad quality (Hughes, 2006). Furthermore, the near-real-time availability of the satellite-based data products makes them suitable for modelling applications where water resources management is crucial and data gathering and quality assurance are cumbersome (Stisen and Sandholt, 2010). The use of satellite-based information to improve spatial rainfall estimates has been widely reported (Hsu et al., 1999; Sorooshian et al., 2000; Grimes and Diop, 2003). Nevertheless, satellites data have biases and random errors that are caused by various factors like sampling frequency, nonuniform field-of-view of the sensors, and uncertainties in the rainfall retrieval algorithms (Nair et al., 2009). It is therefore essential to validate the satellite derived products with conventional rain estimates to quantify the direct usability of the products (Nair et al., 2009).

The Tropical Rainfall Measuring Mission (TRMM) is a joint project between the National Aeronautics and Space Administration (NASA) and the Japan Aerospace Exploratory Agency (JAXA) launched in November 1997 with the specific objectives of studying and monitoring the tropical rainfall (Kummerow et al., 2000; Rozante et al., 2010). It can provide precipitation products with high temporal (3 h) and reasonably high spatial resolution ($0.25° \times 0.25°$) for large-scale distributed hydrological models. There have been numerous attempts to validate TRMM retrievals with ground-based estimates in the tropics and the mid-latitudes (Nair et al., 2009). Nicholson et al. (2003) used gauge data from a network of 920 stations over West Africa to evaluate TRMM (PR, TMI, 3B43) rainfall products for the year 1998. While TRMM PR and TMI products showed a net tendency to overestimate gauge measurements, 3B43 merged product showed an excellent agreement with gauge measurements on monthly to seasonal timescales. Narayanan et al. (2005) validated TRMM 3B42-V5 data with India Meteorological Department (IMD) rain gauge data and showed that the satellite algorithm does not pick up very high and very low daily average rainfalls. Rahman and Sengupta (2007) compared the Global Precipitation Climate Project (GPCP), 3B42-V5 and 3B42-V6 rainfall products with the IMD gridded daily rainfall at grid resolution of $1° \times 1°$ for the monsoon season. Their results showed that GPCP and 3B42-V5 reproduce only the broadest features of the monsoon rainfall, but spatial patterns of 3B42-V6 data show closest agreement with observed patterns of IMD gauge data except over certain places. Stisen and Sandholt (2010) evaluated five satellite-based rainfall estimates with temporal resolution of daily and spatial resolution between 8 and 27 km through their predictive capability in a distributed hydrological model. However, most validation studies are performed at continent/sub-continent or regional scale. Therefore fewer studies deal with the comparison between TRMM rainfall and rain gauge data at catchment scale, and no evaluation of hydrological processes simulation and water balance analysis using TRMM rainfall data in mesoscale catchments which will provide useful information for hydrology studies.

Therefore, the objectives of the study are designed to (1) evaluate and compare the temporal characteristic of daily TRMM rainfall and the spatial distribution of annual rainfall with that of the rain gauge data in a mesoscale catchment located in the lower reaches of the Yangtze River in China. By doing so, different statistical measures are calculated and the correlations of the TRMM rainfall with rain gauge data at monthly time scale are investigated; and (2) cross compare the performance of the TRMM rainfall and rain gauge data in driving the Water Flow Model for Lake Catchment (WATLAC) model (Zhang, 2007; Zhang and Werner, 2009; Zhang and Li, 2009) in simulation of daily and monthly hydrological processes at the catchment. Emphasis was paid to investigate the suitability of the TRMM rainfalls for water balance analysis through a distributed hydrological model at different time scales, although some researchers consider that most satellite-based rainfall estimation techniques are better suited at determining rain/no rain situations compared to actually determining the rainfall amount (Stisen and Sandholt, 2010), and imprecise rainfall amounts and especially biases are critical in water balance studies (Stisen and Sandholt, 2010). This study contributes to the enhancement of knowledge regarding the usefulness of TRMM 3B42-V6 rainfall data in hydrological modelling studies at catchment scale over varying time scales.

The rest of this paper is organized as follows. In the next section we will provide details of the study area and the data used. In Section 3, the concept of WATLAC model is briefly described with the help of cited references. Major results of this study are presented and discussed in Sections 4 and 5 summarizes the conclusions.

2. Study area and data preparation

The Xinjiang catchment (27°33′–28°59′N and 116°23′–118°22′E) is selected as the study area, which is one of the five river catchments of Poyang Lake (the largest freshwater lake in China) basin located in the lower reaches of the Yangtze River (Fig. 1). The catchment above Meigang Hydrological station covers about 15500 km^2 and has a subtropical wet climate characterized by a mean annual precipitation of 1878 mm for the period of 1960–2005 and annual mean temperature of 18 °C. The topography varies from high mountainous and hilly areas (with a maximum elevation of 2138 m.a.s.l) to alluvial plains in the lower reaches of the primary watercourses. The Xinjiang River flows primarily from the east to the west and enters Poyang Lake. The average stream flow at Meigang station for the 1960–2002 period was 578 m^3/s.

Based on the digital elevation model (DEM) data of the catchment which are derived from the National Geomatics Centre of China, the river network and physical boundaries of the catchment are delineated. Landuse map is available from previous studies (Ye et al., 2011a,b) as Fig. 2 shows. In the Xinjiang catchment, forest is the main land use covering 84% of the catchment area, followed by crop land of 10% and Shrubland of 5%. Other land uses such as

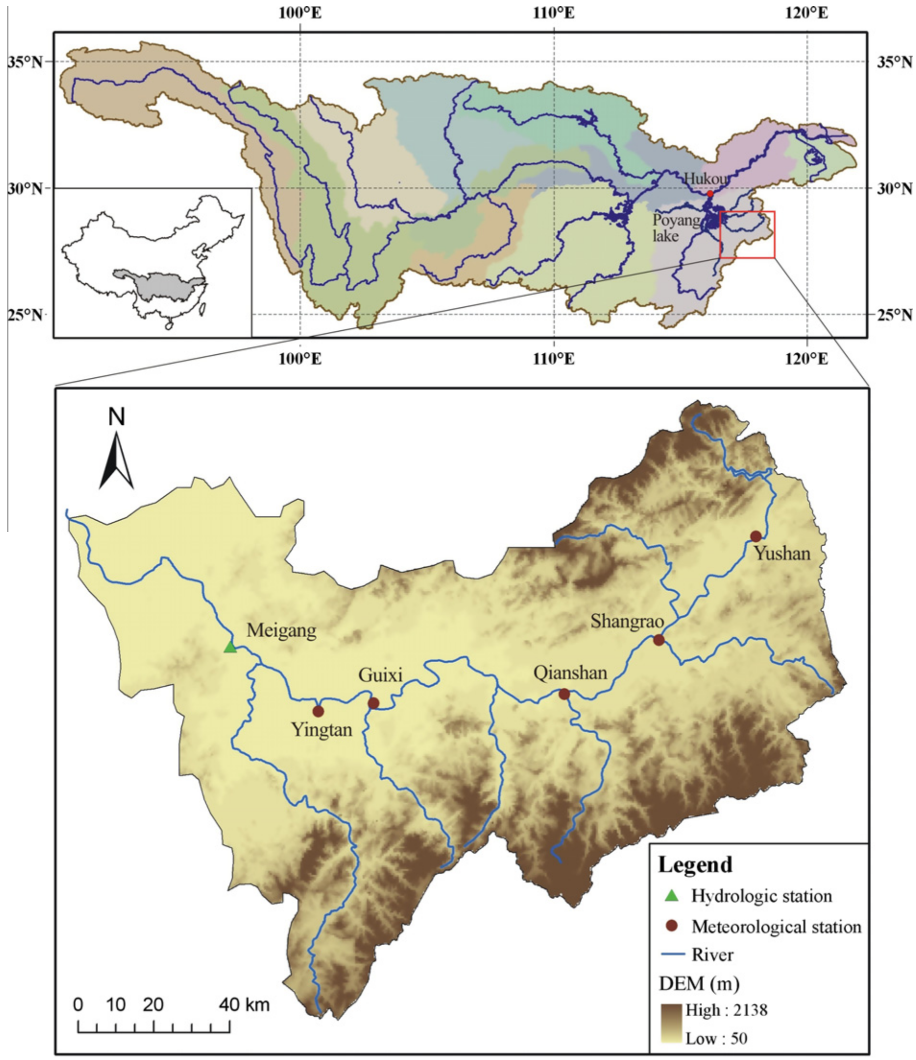

Fig. 1. Location of Xinjiang catchment in Poyang Lake basin and the distribution of stations.

grassland, water bodies and urban are minor with a total area of 1%. Land use condition is simulated in the model through the parameters of maximum canopy interception which is assumed to be linearly proportional to the Leaf Area Index (LAI) (Zhang and Li, 2009). And LAI for each vegetation class can be derived from National Oceanic and Atmospheric Administration/Advanced Very High Resolution Radiometer (NOAA/AVHRR) Normalized Difference Vegetation Index (NDVI) data through the Simple Biosphere Model Version 2 (SiB2) method (Myneni and Williams, 1994; Sellers et al., 1994, 1996; Andersen et al., 2002; Zhou et al., 2006):

$$\mathrm{SR} = \frac{1 + \mathrm{NDVI}}{1 - \mathrm{NDVI}} \tag{1}$$

$$\mathrm{FPAR} = \mathrm{FPAR}_{\min} + (\mathrm{FPAR}_{\max} - \mathrm{FPAR}_{\min})\frac{\mathrm{SR} - \mathrm{SR}_{\min}}{\mathrm{SR}_{\max} - \mathrm{SR}_{\min}} \tag{2}$$

$$\mathrm{LAI} = (1 - F_{cl})\mathrm{LAI}_{\max}\frac{\ln(1 - \mathrm{FPAR})}{\ln(1 - \mathrm{FPAR}_{\max})} + F_{cl}\mathrm{LAI}_{\max}\frac{\mathrm{FPAR}}{\mathrm{FPAR}_{\max}} \tag{3}$$

where SR is the simple ratio of hemispheric reflectance for the NIR (near-infrared) light to that for the visible light, FPAR is the fraction of photo-synthetically active radiation, F_{cl} is the fraction of clumped vegetation, SR_{min} and SR_{max} are SR with 5% and 98% of NDVI population. The values of NDVI at 5% population are adopted from SiB2 for all vegetation types ($\mathrm{NDVI}_{5\%} = 0.039$ globally). $\mathrm{FPAR}_{min} = 0.001$ and $\mathrm{FPAR}_{max} = 0.950$ consider the satellite-sensed NDVI saturation. LAI_{max} is the maximum LAI when the vegetation develops fully.

Some useful parameters for each vegetation class are shown in Table 1 from Zhou et al. (2006).

The soils in the catchment are classified according to the Genetic Soil Classification of China, and soil distributions are obtained from a soil survey completed by the Land Management Bureau of Jiangxi Province, China. Soil types of the catchment are dominated by paddy soil (47%) and red soil (45%); other types include yellow soil (6%), latosol (1%) and a spot of yellow–brown[1] soil (0.7%) and purplish soil (0.3%) as Fig. 3 shows. The properties of every soil type are determined from the soil survey (Shi et al., 2004) and are shown in Table 2, with porosity ranging from 0.48 to 0.50, field capacity from 0.32 to 0.36, and saturated hydraulic conductivity varying from 0.60 to 0.90 m/d.

Satellite-based rainfall data used in this study are TRMM 3B42-V6 daily data from 1 January, 1998 to 31 December, 2003. And for the comparison of rainfall data between TRMM and rain gauges, we also use the rain gauge data from five national meteorological stations namely Yushan, Shangrao, Qianshan, Guixi and Yingtan

[1] For interpretation of color in Figs. 1–3 and 5–7, the reader is referred to the web version of this article.

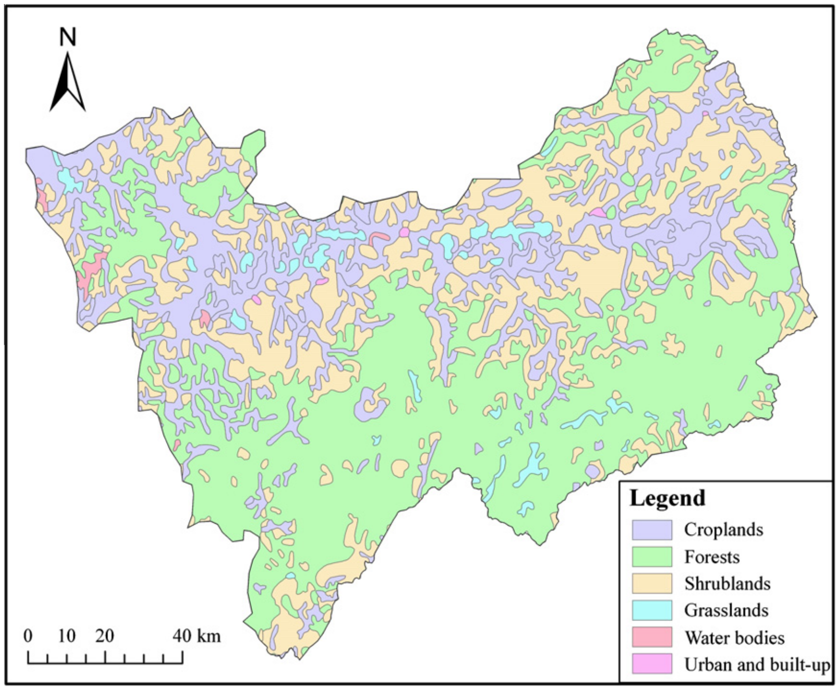

Fig. 2. The landuse map of study area.

Table 1
Landuse threshold parameters from the literatures.

Type	LAI_{max}	F_{cl}	$NDVI_{98\%}$	Root depth (m)	Permeable area (%)	Roughness
Croplands	7.0	0	0.674	0.7	70	0.101
Forests	5.7	0.5	0.721	2.5	60	0.122
Shrublands	3.0	1.0	0.674	1.0	80	0.107
Grasslands	1.8	0	0.674	0.5	90	0.085
Water bodies	–	0	0.674	1.3[a]	5	0.073
Urban and built-up	–	0	0.674	0.1	5	0.047

[a] Root depths for water bodies represent the average water depth (Zhou et al., 2006).

as Fig. 1 shows. Moreover, other meteorological data including daily maximum and minimum temperature, solar radiation, wind speed, and relative humidity are derived from these national stations and used in the study for calculating evapotranspiration and related processes. These data have been widely used for different studies previously and the qualities of the data are quite reliable. We also examined the relation between elevation and rainfall to reflect the difference in mountainous region and in lowlands, but there is no clear evidence that the rainfall changed with elevation in the study region. So, the daily rainfall data are directly interpolated to grid (4 km $\times$ 4 km) for the whole basin with the method of Thiessen polygon to satisfy the requirement of the distributed hydrological model. In addition, the observed daily stream flow from the Meigang gauging station is available to calibrate model parameters and validate the simulation results.

3. Hydrological model

The WATLAC model (Zhang and Werner, 2009; Zhang and Li, 2009), is a grid-based spatially distributed hydrological model with effective computational techniques to simulate complex spatial variability of surface and subsurface flows. The model was designed to simulate processes including canopy interception, overland flow, stream flow routing, unsaturated soil water storage, soil lateral flow, soil water percolation to groundwater and saturated groundwater flow driven by rainfall and evaporation. The land surface (including river networks), unsaturated soil layer and saturated groundwater aquifer were coupled in the model and can reflect the interaction of groundwater and surface water. The most of model parameters can be determined through field survey or literature values and only few parameters need to be estimated through calibration. The WATLAC model has been successfully applied for water balance analysis of Fuxian lake catchment (Zhang and Werner, 2009), surface–groundwater flow interactions modelling of Xitiaoxi catchment (Zhang and Li, 2009) and assessment of the effects of future climate change on catchment discharges and lake water level of Poyang lake (Liu et al., 2009; Ye et al., 2011a). Details of model structure were provided in Zhang and Li (2009) and Zhang and Werner (2009) and therefore only a brief description is given here.

The WATLAC model first calculates the throughfall P_n taking into account canopy interception which will be evaporated back into the atmosphere and the maximum soil water storage S_{max}. Once the S_{max} is filled, the exceeding throughfall becomes the surface runoff. The maximum soil water storage S_{max} is calculated as

$$S_{max} = h_s \cdot \phi \tag{4}$$

where ϕ is the porosity of the soil; h_s is the thickness of the simulated soil layer (mm).

The water that infiltrates into the soil subsequently percolates downwards under gravity to the groundwater table, or flow laterally close to the surface as soil lateral flow, or else it may be evaporated.

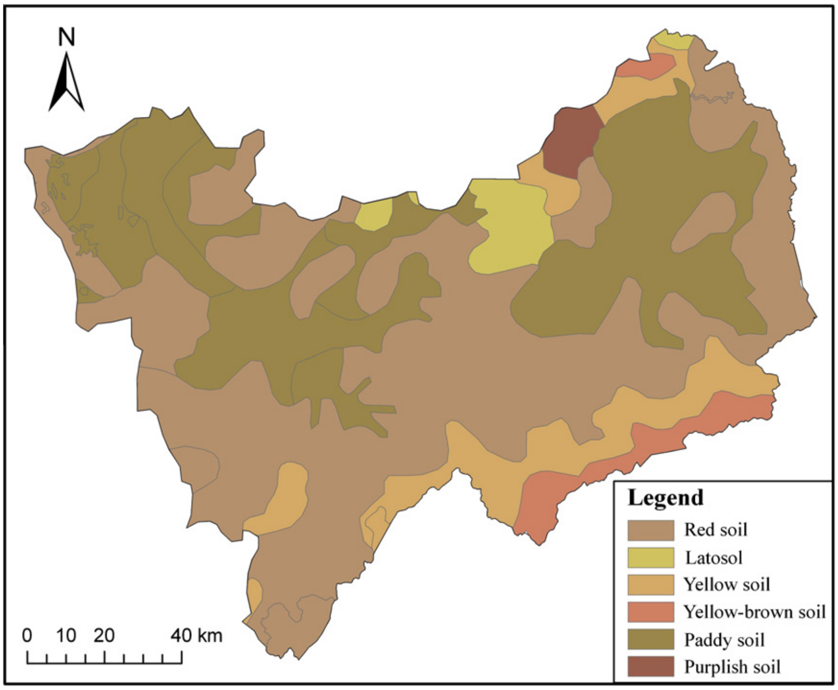

Fig. 3. The soil type map of study area.

Table 2
The property of each soil type from the soil survey.

Soil type	Porosity	Field capacity	Saturated K (m/day)
Red soil	0.48	0.34	0.67
Latosol	0.47	0.34	0.60
Yellow soil	0.50	0.35	0.79
Yellow–brown soil	0.50	0.36	0.90
Paddy soil	0.46	0.33	0.63
Purplish soil	0.48	0.32	0.86

The groundwater recharge rate R_G, is computed as a function of the drainable soil water, saturated soil hydraulic conductivity and shallow aquifer conductivity, similar to that in Neitsch et al. (2002). An empirical parameter β_1 ($\beta_1 \geqslant 0$) is introduced in the computation, through which the magnitude of the groundwater recharge can be adjusted and a larger value will result in a greater groundwater recharge rate. Generally, it should be set in the range of 0.0–10.0 and can be best estimated in model calibration.

The soil lateral flow R_L is calculated using a function of soil drainable water, soil hydraulic conductivity, soil slope length and slope gradient as that used in SWAT (Neitsch et al., 2002). Also, an empirical parameter β_2 ($\beta_2 \geqslant 0$) is introduced to reflect the magnitude of soil lateral value. This parameter is usually in the range of 0.0–10.0 for most cases and can only be estimated in model calibration.

Actual evapotranspiration calculation adopts the same approach as that in USACE (2000), i.e., the total evapotranspiration is a sum of various components from canopy storage, soil storage and shallow groundwater. The potential evapotranspiration used as the up limit of the actual evapotranspiration is calculated using the Penman–Monteith approach (Xu et al., 2006).

Overland flow routes are generated from DEM by the D-8 method considering time lag effects when the overland flow is transferred from overland to known waterways. Stream flow routing is simulated using the Muskingum method. The saturated groundwater flow is simulated through MODFLOW-2005 (Harbaugh, 2005) which was integrated in WATLAC and can achieve the interaction with surface water flow, i.e. on the one hand, the groundwater recharge calculated from the surface water model is passed to the MODFLOW for groundwater flow modelling; on the other hand, groundwater table simulated from MODFLOW is used in surface water model to update the thickness of the soil column (Zhang and Li, 2009).

The model parameters are automatically optimized by the PEST (Parameter ESTimation) optimization tool (Doherty, 2004). PEST is a robust and efficient model-independent parameter estimation software, which uses the Gauss–Marquardt–Levenberg algorithm to identify the parameter set that gives the least sum of square difference between simulated and observed data, and has been widely used for groundwater-surface water optimization problems (Keating et al., 2003). The model performance is evaluated using statistical analyses of model outputs. Evaluation criteria, e.g., Nash–Sutcliffe efficiency (E_{ns}) and determination coefficient (R^2) are used to measure the capability and reliability of the model in describing the observed processes. In addition, for evaluation of systematic errors in model simulation, the relative runoff depth error (DE) is also analysed. The values of E_{ns} and DE are calculated, respectively, as

$$E_{ns} = 1 - \sum_{i=1}^{n}(Qobs_i - Qsim_i)^2 / \sum_{i=1}^{n}(Qobs_i - \overline{Q}obs)^2 \tag{5}$$

$$DE = \sum_{i=1}^{n}(Qsim_i - Qobs_i) / \sum_{i=1}^{n} Qobs_i \times 100\% \tag{6}$$

where $Qobs_i$ is the observed stream flow at step i; $Qsim_i$ is the simulated stream flow at step i; and $\overline{Q}obs$ is the mean observed stream flow over all time steps; and n is the total time step.

4. Results and discussions

4.1. Validation of TRMM rainfall with rain gauges data

For the comparison of rainfall data between rain gauges and TRMM, we first analyse several statistical indices of two types of

Table 3
Comparison of statistical indexes between averaged TRMM rainfall and rain gauges rainfall.

Year	Areal average (mm/d)		Standard deviation (mm)		Max. daily rainfall (mm/d)		Max. 5-day rainfall (mm/5d)		Annual rainfall (mm/y)	
	Gauging	TRMM	Gauging	TRMM	Gauging	TRMM	Gauging	TRMM	Gauging	TRMM
1998	7.4	6.3	17.9	15.9	146	158	478	312	2702	2281
1999	5.9	5.3	14.2	11.3	148	70	232	174	2176	1930
2000	5.7	4.9	15.6	10.7	175	82	296	157	2075	1788
2001	4.9	5.1	10.3	10.9	103	87	154	117	1801	1844
2002	5.6	6.1	11.5	11.9	71	78	205	231	2057	2234
2003	4.1	4.1	10.6	10.7	89	115	181	252	1477	1506

rainfall, and the results are shown in Table 3. Areal average rainfall is an important and useful index to reflect the precision of rainfall amount. The areal average rainfalls, estimated from rain gauges data using the Thiessen polygon interpolation method, are 4.1–7.4 mm/d in 1998–2003 and 4.1–6.3 mm/d for TRMM data in the same period. The differences are small and at an acceptable extent. But the areal average rainfalls from TRMM data are smaller than those from rain gauges data in 1998–2000, and the opposite is true in 2001–2003. A comparison of standard deviations calculated from the two data sets shows the same situations as those for areal

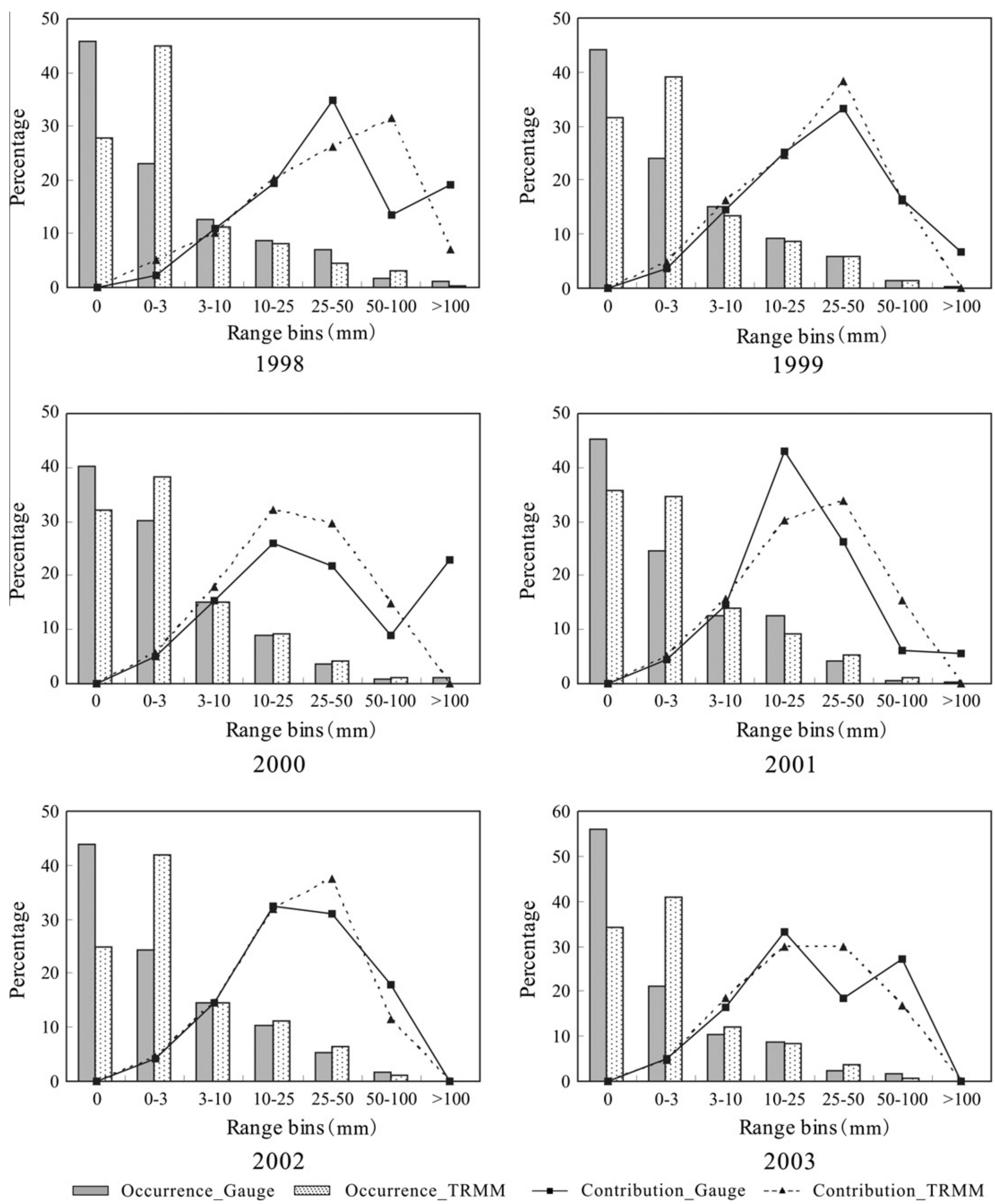

Fig. 4. Distribution of daily rainfall in different rainfall classes and their relative contributions to the total rainfall in different years.

average rainfall. The difference in the extreme rainfall is larger than that in the mean values and the standard deviations. The maximal daily rainfall from rain gauges data are 146 mm, 148 mm, 175 mm, 103 mm, 70 mm and 89 mm, respectively in 1998–2003, while they are 158 mm, 70 mm, 82 mm, 87 mm, 78 mm and 115 mm, respectively for TRMM data. It is shown that the maximal 5-day rainfalls from TRMM data are lower than that from rain gauges data except in 2002 and 2003. As for the annual rainfall totals, the TRMM data are smaller than rain gauges data in 1998–2000, but larger than the latter in 2001–2003.

Fig. 4 shows the intensity distributions of daily rainfall in different classes and their contributions to the total rainfall in different years. It is seen that non rainy has the largest occurrence, occurring almost half of the total days and the second largest class is 0 < rainfall ⩽ 3 mm, occurring about 20–30% of the total days in gauges rainfall. While, the statistics for TRMM rainfall are different from gauge rainfall, the largest rainfall occurrence is 0 < rainfall ⩽ 3 mm, accounting for about 40% of the total days and followed by non rainy (accounting for about 30%). That is to say more non rainy days are recorded in rain gauges and more days in small rainfall class (0 < rainfall ⩽ 3 mm) in TRMM data, which is partly because the rain gauges only refer to five specific points and many small rainfall (⩽0.01 mm) occurred in some days are regarded as non rainy in rain gauge situation. The sum of the first two classes, i.e. non rainy and small rain classes, gives the similar percentage (≈70%) for both TRMM data and gauge data. It can also be seen that although the occurrences of small rain (0 < rainfall ⩽ 3 mm) are as high as 40–50% of the total days, the contribution to the total rainfall amount is only about 4% in both rainfall data.

It is important to note that the high rainfall ranges play a significant role in contributing rain amount to the total rainfall. The high rainfall class (>50 mm) occurs only about 1.1% (maximal 3% in 1998) of the total days and contributes to 22.4% in average values (maximal 32.5% in 1998) of the total rainfall for rain gauge data and 15% (maximal 38.3% in 1998) for TRMM data. This kind of information is essential because thunder showers cause the geographical slides and flash floods and hence threaten the economy and human life (Varikoden et al., 2010). The occurrences of the middle class rainfall ranges (3 mm < rainfall ⩽ 50 mm) are generally equivalent (accounting for 27.7% in average) for rain gauge and TRMM rainfall data, but with different contribution rates to the total rainfall. For the class of 3–10 mm, the statistics for TRMM rainfall match well with its counterpart in every year. And for the range of 10–25 mm, the contribution rate is larger in 2000 and smaller in 2001 than that of rain gauge rainfall, and in other years they are nearly equivalent.

In order to evaluate the correlation of the two data sets, the scatter plots of monthly TRMM rainfall against rain gauges rainfall data are shown in Fig. 5, and the comparison is made for the five national meteorological stations and the areal average data of the nearest TRMM pixel. It is seen that the good linear relationships between the nearest TRMM pixel data and rain gauge data are presented in every stations, with the highest determination coefficient (R^2) of 0.89 for Yushan station. The R^2 values for the rest stations

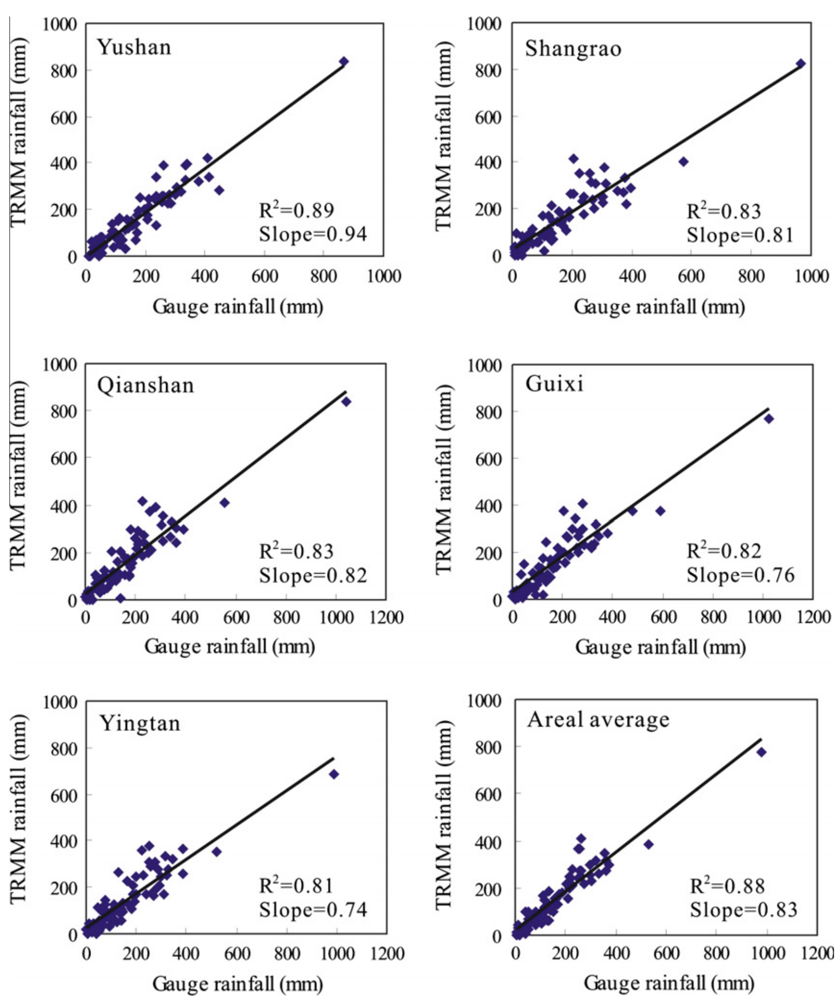

Fig. 5. Scatter plots of monthly rainfall from TRMM and rain gauges data for the five national meteorological stations and the areal average data.

Table 4
Estimated parameters for two scenarios and the 95% confidence intervals for each parameter.

Parameter	Description	Initial values	Lower bound	Upper bound	Optimal values	
					Scenario 1	Scenario 2
e	A parameter of Muskingum method (Weighting factor) (dimensionless)	0.107	0.05	0.5	0.138 ± 0.049	0.081 ± 0.022
k	A parameter of Muskingum method (Travel time of flood) (day)	1.329	0.5	2.0	1.44 ± 0.082	1.756 ± 0.075
β_1	An empirical coefficient for groundwater recharge (dimensionless)	0.753	0.01	10.0	0.387 ± 0.098	0.928 ± 0.211
β_2	An empirical coefficient for soil lateral flow (dimensionless)	0.884	0.01	10.0	0.828 ± 0.148	0.184 ± 0.089
β_3	An empirical coefficient for infiltration (dimensionless)	0.081	0.01	10.0	0.117 ± 0.004	0.019 ± 0.007

Table 5
Comparison of the model performance using TRMM rainfall and rain gauge rainfall (Values in the gray areas are calibration results).

Year	First scenario						Second scenario					
	Gauge rainfall-based model			TRMM rainfall-based model			Gauge rainfall-based model			TRMM rainfall-based model		
	E_{ns}	DE (%)	R^2	E_{ns}	DE (%)	R^2	E_{ns}	DE (%)	R^2	E_{ns}	DE (%)	R^2
1998	0.96	−4.33	0.96	0.80	−17.37	0.83	0.96	−1.68	0.96	0.81	−16.45	0.84
1999	0.92	−4.93	0.92	0.49	−16.59	0.50	0.90	−4.59	0.91	0.48	−16.78	0.49
2000	0.89	−1.87	0.91	0.64	−21.33	0.67	0.87	7.01	0.89	0.66	−12.62	0.68
2001	0.81	−7.64	0.83	0.53	5.86	0.68	0.78	−4.81	0.81	0.56	6.34	0.70
2002	0.89	2.23	0.90	0.74	17.6	0.76	0.89	−2.65	0.90	0.75	12.23	0.74
2003	0.87	17.41	0.92	0.43	26.36	0.70	0.87	16.41	0.91	0.51	23.61	0.71
1998–2003	0.93	−0.97	0.92	0.70	−3.97	0.70	0.92	0.49	0.91	0.71	−3.66	0.71

vary from 0.81 for Yingtan station to about 0.83 for other 3 stations. As for areal average, the R^2 value is as high as 0.88. But the slope of regression line ranges between 0.74 for Yingtan and 0.94 for Yushan, and 0.83 for areal average dataset. These values indicate that the TRMM satellite tends to underestimate the monthly rainfall in this area. In general, the TRMM satellite captures the signal of rainfall well in comparison with the rainfall measurement from the manual rain gauges situated in different locations of the Xinjiang catchment, and the systemic errors are also obvious at monthly time step.

4.2. Hydrological processes simulation

The study area was discretized into a number of square grids (4 km × 4 km) considering the heterogeneity of the basin's topography and the stream flow simulation was carried out using the WATLAC model from 1 January 1998 to 31 December 2003. From the experiences of the previous studies and in order to maintain the physical meanings of parameters, in this study, the most physical parameters of WATLAC including the parameters describing the properties of landuse, soil and river, etc. are determined prior from the survey database and literature values according to the digital soil and land cover maps. Several empirical parameters such as β_1, β_2 and β_3 for groundwater recharge estimation, soil lateral flow calculation and soil infiltration respectively and e and k parameters in the Muskingum method are automatically optimized by the PEST (Doherty, 2004). The initial parameter values are gained from the previous calibration and the lower and upper bounds for each parameter are determined according to the physical meanings and experiences. In this section, the sum of squared residuals is used as the objective function and the optimization process is performed in two scenarios: In the first scenario, the daily rain gauge rainfalls are used to feed the model and to optimize the parameter values, and then the model is run again using daily TRMM rainfalls with unaltered model parameter values in the same periods. The simulation results of the two data sets are compared. In the second scenario, the daily TRMM rainfalls are used to drive the WATLAC model and to optimize the parameter values, and then the model is run using the rain gauge rainfalls and the results are compared. The results of parameters' optimization and the summary values of evaluation criteria of model performance using two types of rainfall data are shown in Tables 4 and 5, respectively.

It is seen from Table 4 that the optimized parameter values and their 95% confidence intervals for both scenarios (although somehow different as expected) are well located within the bounds. Table 5 reveals that the model using conventional rain gauge data produces an overall good fit in the first scenario. The E_{ns} ranges between 0.81 and 0.96, with an average of 0.93. The relative runoff depth errors, except in 2003, are less than 8%. In addition, the relatively high values of R^2 (from 0.83 to 0.96) show that the model describes the variation of the observed stream flow well. So, based on the presented results, the model is believed to be robust and provides a sound basis for testing the precision and applicability of TRMM rainfall. However, the results for TRMM rainfall data are discontented. The E_{ns} values, except in 1998, are not higher than 0.74 and the R^2 ranges from 0.50 to 0.83. The precisions of the simulated runoff volume are relatively low with the relative runoff depth errors ranges from −21.33% to 26.36%. In the second scenario, it can be seen from Table 5 that the TRMM rainfall-based model calibration produces a slightly improved results with E_{ns} ranges between 0.48 and 0.81 and the determination coefficients R^2 are mildly increased. The relative runoff depth errors are also improved from that of the first scenario. At the same time, the performance of the gauge rainfall-based model is still satisfactory. The E_{ns} values are over 0.8 in five years and the average relative runoff depth errors is 0.49%; the determination coefficients R^2 also gain the relatively high values. It is obvious that the relative runoff depth errors are large for TRMM rainfall case in both scenarios and have the same traits that the model underestimates the runoff volumes in 1998–2000 but overestimates them in 2001–2003. This shortcoming originates from the errors of rainfall estimation through TRMM satellite data as discussed in Table 3.

Fig. 6 shows the comparison of the observed and simulated daily stream flow hydrographs which are produced by the gauge rainfall-based model and TRMM rainfall-based model respectively with their own optimal parameter values. It is seen that the simulated stream flow hydrographs with rain gauges data demonstrated a closer agreement with the observed hydrographs, while the model simulation using TRMM daily rainfall behaved less well and there was a tendency for the model to miss the extreme peak flows. This attributes to the low precision of TRMM rainfall data in matching the maximal rainfalls as discussed before. It seems that the TRMM rainfall data are unsuited for daily stream flow simulation in this study area with desired precision.

Subsequently, we also examine the precision of the model using TRMM rainfall data for monthly stream flow simulation. The evaluations of model performance using TRMM rainfall and rain gauge rainfall for the complete simulation periods and the comparison of the observed and simulated monthly hydrographs are shown in Tables 6 and 7, respectively. It can be seen from Table 6 that the gauge rainfall-based model performs as well as before, with the E_{ns} of 0.97, the DE of −0.89% and the R^2 of 0.97; at the same time, it is encouraging that the model using TRMM rainfall data also gains the satisfying results, the E_{ns} and R^2 are 0.86 and the DE is −4.1%. It is obvious from Fig. 7 that the simulated monthly hydrographs generally match well with the observed ones and describe the seasonal variations well, although it slightly underpredicts some peak flows when using TRMM rainfall data. From the results of monthly simulation we believed that it is feasible to use TRMM rainfall data for monthly discharges simulation, and it has potential to be a suitable data source for the data-poor or ungauged basins, particularly for the large basins in developing countries or remote locations.

Table 6
The model performance using TRMM rainfall and rain gauge rainfall at monthly time step.

Data sets	E_{ns}	DE (%)	R^2
Gauge rainfall-based model	0.97	−0.89	0.97
TRMM rainfall-based model	0.86	−4.1	0.86

4.3. Water balance analysis

In addition to the comparison of stream flow hydrographs, water balance result is another important indicator for testing the validity of rainfall data. So, we examine the difference of water balance components further from monthly stream flow simulations using rain gauges and TRMM rainfall. According to the above modelling results, comparisons of the averaged water balance components from 1998 to 2003 are shown in Table 7. In the model, the water balance partitions the precipitation into canopy interception, soil evaporation, surface runoff, groundwater recharge (includes base flow) and so on. In the rain gauge driven calculation, 10.5% of precipitation is intercepted by canopy which is exhausted through evaporation, while the rate is 11.3% in TRMM rainfall data case. The proportion of soil evaporation is 22.7% and 23.8% respectively in gauge rainfall and TRMM rainfall case. Groundwater recharge is a large component and determines the amount of base flow. Although the volume of precipitation has a markable differ-

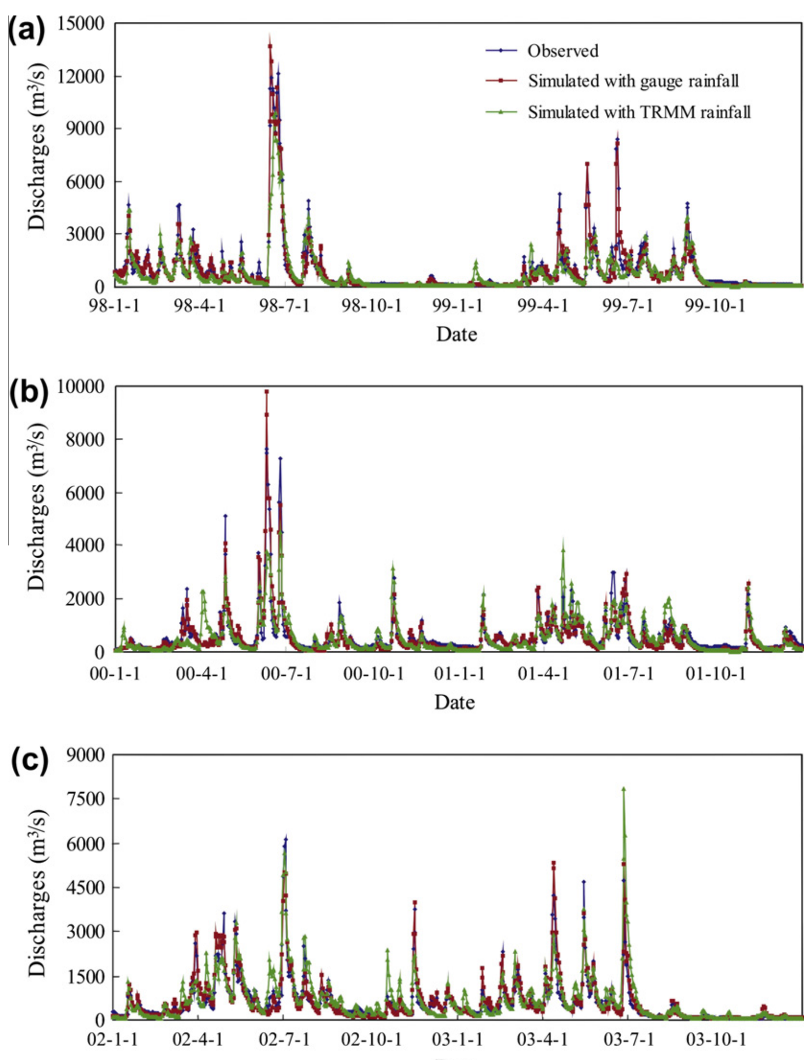

Fig. 6. Comparison of the observed and simulated daily hydrographs at Meigang station.

Table 7
Comparison of the water balance components using rain gauges and TRMM rainfall.

Components	Gauge rainfall-based model			TRMM rainfall-based model		
	Volume (mm/y)	Percentage of precipitation (%)	Percentage of total runoff (%)	Volume (mm/y)	Percentage of Precipitation (%)	Percentage of total runoff (%)
Precipitation	2049			1930		
Canopy interception	216	10.5		218	11.3	
Soil evaporation	466	22.7		460	23.8	
Groundwater recharge	434	21.2		451	23.4	
Total runoff	1222	59.6		1182	61.2	
Surface runoff	840		68.7	774		65.5
Base flow	382		31.3	408		34.5

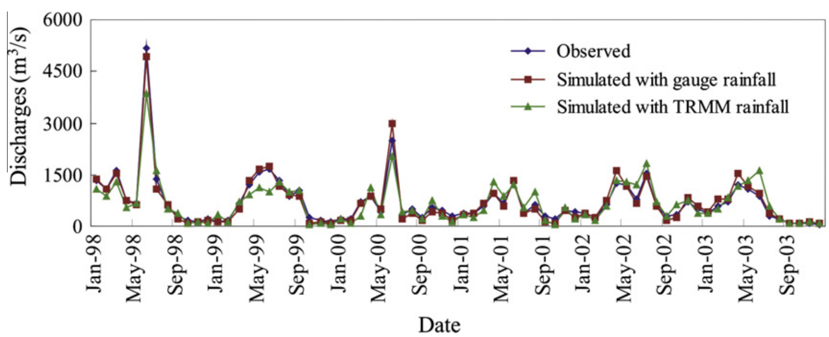

Fig. 7. Comparison of the observed and simulated monthly hydrographs at Meigang station.

ence (2049 mm/y and 1930 mm/y) in different rainfall cases, the estimated amounts of groundwater recharge are very similar (434 mm and 451 mm). As for the total runoff, more precipitation is distributed into runoff in gauge rainfall case (1222 mm) than in TRMM rainfall case (1182 mm). In fact, this difference is mainly produced by surface runoff estimation which is 840 mm for gauge rainfall case and 774 mm for TRMM rainfall case and the proportion to the total runoff are 68.7% and 65.5%, respectively, while the differences of base flow volume are small (382 mm and 408 mm). The general conclusion that can be drawn from Table 7 is that the different rainfall data sources can change the volume value and proportion of water balance components, especially for runoff and its compositions.

5. Conclusions

This paper compares the difference of TRMM rainfall with rain gauges data at daily and monthly time steps and evaluates the usefulness of the TRMM rainfall for hydrological processes simulation and water balance analysis at the Xinjiang catchment, China. The results reveal that the differences of areal average rainfall calculated from two rainfall sources are small and in an acceptable extent, but larger difference exists for the maximal daily and maximal 5-day rainfalls. The occurrences of the middle class rainfall ranges (3 mm < rainfall ⩽ 50 mm) are generally equivalent for rain gauge data and TRMM rainfall data, but their contributions to the total rainfall are different. So, the daily TRMM rainfall data are better at determining rain occurrence and mean values than at determining the rainfall extremes. Moreover, the good linear relationships of the monthly TRMM rainfall with monthly rain gauges rainfall data are presented in every rain gauge stations. The simulation of daily hydrological processes shows that the WATLAC model using conventional rain gauge data produces an overall good fit, but the results for TRMM rainfall data are discontented at daily time step. The statistical results imply that the TRMM rainfall data are unsuited for daily stream flow simulation in this study area with good precision. But, a good performance using TRMM rainfall data for monthly stream flow simulation can be achieved. The comparison of water balance components using two type rainfalls shows that the different rainfall data sources can change, to some extent, the volume value and proportion of water balance components, especially for runoff and its compositions.

In conclusion, it can be said that the satellite-based rainfall, e.g. TRMM data, have good potential for useful application to hydrological simulation and water balance calculations at monthly or seasonal time steps, which is a useful merit for regions where rain gauge observations are sparse or of bad quality. However, several shortcomings, such as the TRMM overestimates the rainfall in some years and areas and underestimates in other years and areas, and failed to detect the extreme rainfall, reduced the accuracy of stream flow simulation at short time steps and other applications including drought monitoring and flood forecasting.

The above mentioned conclusions indicate that it is necessary to further develop algorithms of satellite-based rainfall estimation in terms of both the accuracy and spatiotemporal resolutions of rainfall estimates (Li et al., 2009). And the extensive efforts of satellite-based products evaluation need to continue in different climatic areas using different sensors and retrieval methods. A thorough understanding of the errors in satellite rainfall is needed which is critical to any analysis of its skill in hydrologic predictions (Pan et al., 2010). Moreover, hydrologists should develop innovative ways to use the current generation of satellite-based rainfall, notwithstanding their limitations, to augment traditional models and methods (Tang et al., 2010).

Acknowledgments

The authors would like to thank the two anonymous reviewers and the editor who helped us improving the quality of original manuscript. This work is jointly funded by the Knowledge Innovation Program of Chinese Academy of Sciences (KZCX2-YW-Q10-3), the National Basic Research Program of China (973 Program) (2012CB417003), the Knowledge Innovation Program of Chinese Academy of Sciences (KZCX2-YW-337), the Ministry of Water Resources' special funds for Scientific Research on Public Causes (No. 200901042), the National Natural Science Foundation of China (41101024 and 40871026) and the Science Foundation of Nanjing Institute of Geography and Limnology, Chinese Academy of Sciences (NIGLAS2010XK02 and NIGLAS2010QD02).

References

Abbott, M.B., Refsgaard, J.C., 1996. Distributed Hydrological Modelling. Kluwer Academic Publishers., Dordrecht, Netherlands.
Andersen, J., Dybkjaer, G., Jensen, K.H., Refsgaard, J.C., Rasmussen, K., 2002. Use of remotely sensed precipitation and leaf area index in a distributed hydrological model. Journal of Hydrology 264, 34–50.
Brown, P.J., Le, N.D., Zidek, J.V., 1994. Multivariate spatial interpolation and exposure to air pollutants. Canadian Journal of Statistics 22 (4), 489–509.
Creutin, J.D., Obled, C., 1982. Objective analyses and mapping techniques for rainfall fields: an objective comparison. Water Resources Research 18, 413–431.
Doherty, J., 2004. PEST: Model-independent parameter estimation. User manual, fifth ed. Watermark Numerical Computing, Brisbane, QLD, Australia.
Gourley, J.J., Vieux, B.E., 2006. A method for identifying sources of model uncertainty in rainfall-runoff simulations. Journal of Hydrology 327 (1–2), 68–80.
Grimes, D., Diop, M., 2003. Satellite-based rainfall estimation for river flow forecasting in Africa: Part 1. Rainfall estimates and hydrological forecasts. Hydrological Sciences Journal 48 (4), 567–584.
Guillermo, Q., Tabios III, G.Q., Salas, J.D., 1985. A comparative analysis of techniques for spatial interpolation of precipitation. Journal of the American Water Resources Association 21, 365–380.
Haberland, U., 2007. Geostatistical interpolation of hourly precipitation from raingauges and radar for a large-scale rainfall event. Journal of Hydrology 332, 144–157.
Harbaugh, A.W., 2005. MODFLOW-2005. The US Geological Survey modular groundwater model-the Groundwater Flow Process. US Geological Survey Techniques and Methods 6-A16.
He, X., Vejen, F., Stisen, S., Sonnenborg, T.O., Jensen, K.H., 2011. An operational weather radar-based quantitative precipitation estimation and its application in catchment water resources modeling. Vadose Zone Journal 10 (1), 8–24.
Hsu, K., Gupta, H.V., Gao, X., Sorooshian, S., 1999. Estimation of physical variables from multi-channel remotely sensed imagery using a neural network: application to rainfall estimation. Water Resources Research 35 (5), 1605–1618.
Hughes, D.A., 2006. An evaluation of the potential use of satellite rainfall data for input to water resource estimation models in southern Africa. IAHS Publication 308, 75–80.
Keating, E.H., Vesselinov, V.V., Kwicklis, E., Lu, Z.M., 2003. Coupling basin and site-scale inverse models of the Espanola aquifer. Ground Water 41, 200–211.
Kibria, B.M.G., Sun, L., Zidek, J.V., Le, N.D., 2002. Bayesian spatial prediction of random space-time fields with application to mapping PM2.5 exposure. Journal of the American Statistical Association 97, 112–124.
Kummerow, C., Simpson, J., Thiele, O., Barnes, W., Chang, A.T.C., Stocker, E., Adler, R.F., Hou, A., Kakar, R., Wentz, F., Ashcroft, P., Kozu, T., Hong, Y., Okamoto, K., Iguchi, T., Kuroiwa, H., Im, E., Haddad, Z., Huffman, G., Ferrier, B., Olson, W.S., Zipser, E., Smith, E.A., Wilheit, T.T., North, G., Krishnamurti, T., Nakamura, K., 2000. The status of the tropical rainfall measuring mission (TRMM) after two years in orbit. Journal of Applied Meteorology 39 (1), 1965–1982.
Kurtzman, D., Navon, S., Morin, E., 2009. Improving interpolation of daily precipitation for hydrologic modelling: spatial patterns of preferred interpolators. Hydrological Processes 23, 3281–3291.
Le, N.D., Sun, W., Zidek, J.V., 1997. Bayesian multivariate spatial interpolation with data missing by design. Journal of the Royal Statistical Society. Series B: Statistical Methodology 59, 501–510.
Li, L., Yang, H., Wang, J.H., Robert, F.A., Frederick, S.P., Shahid, H., Daniel, I., Tesfaye, K., Lawrence, O., 2009. Evaluation of the real-time TRMM-based multi-satellite precipitation analysis for an operational flood prediction system in Nzoia Basin, Lake Victoria, Africa. Nat Hazards 50, 109–123.
Liu, J., Zhang, Q., Zuo, H.J., Jin, X.L., Li, L.J., Ye, X.C., 2009. A surface runoff model for Lake Poyang watershed. Journal of Lake Sciences 21 (4), 570–578 (in Chinese).
Myneni, R.B., Williams, D.L., 1994. On the relationship between FPAR and NDVI. Remote Sensing of Environment 49, 200–211.
Nair, S., Srinivasan, G., Nemani, R., 2009. Evaluation of multi-satellite TRMM derived rainfall estimates over a Western State of India. Journal of the Meteorological Society of Japan 87 (6), 927–939.
Narayanan, M.S., Shah, S., Kishtawal, C.M., Sathiyamoorthy, V., Rajeevan, M., Kriplani, R.H., 2005. Validation of TRMM merge daily rainfall with IMD raingauge analysis over Indian land mass. Technical Report, Space Applications Centre, Ahmedabad, India.
Neitsch, S.L., Arnold, J.G., Kiniry, J.R., Williams, J.R., King, K.W., 2002. Soil and water assessment tool theoretical documentation, version 2000. Texas Water Resources Institute, College Station, Texas.
Nicholson, S.E., Some, B., McCollum, J., Nelkin, E., Klotter, D., Bere, Y., Diallo, B.M., Gaye, I., Kpabeba, G., Ndiaye, O., Noukpozounkou, J.N., Tanu, M.M., Thiam, A., Toure, A.A., 2003. Validation of TRMM and other rainfall estimates with a high-density gauge dataset for West Africa: Part II. Validation of TRMM rainfall products. Journal of Applied Meteorology 42, 1355–1368.
Pan, M., Li, H., Wood, E., 2010. Assessing the skill of satellite-based precipitation estimates in hydrologic applications. Water Resources Research 46 (9), W09535. doi:10.1029/2009WR008290.
Rahman, H., Sengupta, D., 2007. Preliminary comparison of daily rainfall from satellites and indian gauge data. CAOS Technical Report No. 2007AS1, Centre for Atmospheric and Oceanic Sciences, Indian Institute of Science, Bangalore-12.
Rozante, J.R., Moreira, D.S., de Goncalves, L.G.G., Vila, D.A., 2010. Combining TRMM and surface observations of precipitation: technique and validation over South America. Weather and Forecasting 25 (3), 885–894.
Sawunyama, T., Hughes, D.A., 2008. Application of satellite-derived rainfall estimates to extend water resource simulation modelling in South Africa. Water SA 34, 1–9.
Sellers, P.J., Tucker, P.J., Collatz, G.J., Los, S.O., Justice, C.O., Dazlich, D.A., Randall, D.A., 1994. A global 1 degree by 1° NDVI data set for climate studies. Part 2: The generation of global fields of terrestrial biophysical parameters from NDVI. International Journal of Remote Sensing 15 (17), 3519–3545.
Sellers, P.J., Los, S.O., Tucker, C.J., Iustice, C.O., Dazlich, D.A., Collatz, G.J., Randall, D.A., 1996. A revised land surface parameterization (SiB2) for atmospheric GCMs. Part II: The generation of global fields of terrestrial biophysical parameters from satellite data. Journal of Climate 9, 706–737.
Shi, X.Z., Yu, D.S., Warner, E.D., 2004. Soil database of 1:1000,000 digital soil survey and reference system of the Chinese Genetic Soil Classification System. Soil Survey Horizons 45 (4), 129–136.
Skaugen, T., Andersen, J., 2010. Simulated precipitation fields with variance-consistent interpolation. Hydrological Sciences Journal 55 (5), 676–686.
Sorooshian, S., Hsu, K., Gao, X., Gupta, H.V., Imam, B., Braithwaite, D., 2000. Evaluation of PERSIANN system satellite-based estimates of tropical rainfall. Bulletin of the American Meteorological Society 81 (9), 2035–2046.
Stisen, S., Sandholt, I., 2010. Evaluation of remote-sensing-based rainfall products through predictive capability in hydrological runoff modeling. Hydrological Processes 24 (7), 879–891.
Taesombat, W., Sriwongsitanon, N., 2009. Areal rainfall estimation using spatial interpolation techniques. ScienceAsia 35, 268–275.
Tang, Q.H., Michael, D., Dennis, P.L., Yang, H., 2010. Satellite-based observations of hydrological processes. International Journal of Remote Sensing 31 (14), 3661–3667.
US Army Corps of Engineers (USACE), March 2000. Hydrologic Modeling System HEC-HMS. Technical Reference Manual. Hydrologic Engineering Center, Davis, CA 95616-4687, USA.
Varikoden, H., Samah, A.A., Babu, C.A., 2010. Spatial and temporal characteristics of rain intensity in the peninsular Malaysia using TRMM rain rate. Journal of Hydrology 387, 312–319.
Xu, C.Y., Gong, L., Jiang, T., Chen, D., Singh, V.P., 2006. Analysis of spatial distribution and temporal trend of reference evapotranspiration and pan evaporation in Changjiang (Yangtze River) catchment. Journal of Hydrology 327, 81–93.
Ye, X.C., Zhang, Q., Bai, L., Hu, Q., 2011a. A modeling study of catchment discharge to Poyang Lake under future climate in China. Quaternary International 244 (2), 221–229.
Ye, X.C., Zhang, Q., Viney, N.R., 2011b. The effect of soil data resolution on hydrological processes modelling in a large humid watershed. Hydrological Processes 25 (1), 130–140.
Zhang, Q., 2007. Coupled simulation of surface and subsurface runoffs for lake catchments. Progress in Geography 26 (5), 1–10 (in Chinese).
Zhang, Q., Li, L.J., 2009. Development and application of an integrated surface runoff and groundwater flow model for a catchment of Lake Taihu watershed, China. Quaternary International 208 (1–2), 102–108.
Zhang, Q., Werner, A.D., 2009. Integrated surface-subsurface modeling of Fuxianhu Lake catchment, Southwest China. Water Resources Management 23, 2189–2204.
Zhou, M.C., Ishidaira, H., Hapuarachchi, H.P., Magome, J., Kiem, A.S., Takeuchi, K., 2006. Estimating potential evapotranspiration using Shuttleworth-Wallace model and NOAA-AVHRR NDVI data to feed a distributed hydrological model over the Mekong River basin. Journal of Hydrology (1–2), 151–173.